

Ab Initio Theory of Scattering-Independent Anomalous Hall Effect

Jürgen Weischenberg,¹ Frank Freimuth,¹ Jairo Sinova,² Stefan Blügel,¹ and Yuriy Mokrousov^{1,*}

¹*Peter Grünberg Institut & Institute for Advanced Simulation,
Forschungszentrum Jülich and JARA, 52425 Jülich, Germany*

²*Department of Physics, Texas A&M University, College Station, Texas 77843-4242, USA*

(Dated: June 2, 2018)

We report on first-principles calculations of the side-jump contribution to the anomalous Hall conductivity (AHC) directly from the electronic structure of a perfect crystal. We implemented our approach for a short-range scattering disorder model within the density functional theory and computed the full scattering-independent AHC in elemental bcc Fe, hcp Co, fcc Ni, and L1₀ FePd and FePt alloys. The full AHC thus calculated agrees systematically with experiment to a degree unattainable so far, correctly capturing the previously missing elements of side-jump contributions, hence paving the way to a truly predictive theory of the anomalous Hall effect and turning it from a characterization tool to a probing tool of multi-band complex electronic band structures.

PACS numbers: 72.25.Ba, 72.15.Eb, 71.70.Ej

The anomalous Hall effect (AHE) in ferromagnets is one of the most celebrated transport phenomena in solid-state physics [1]. It has been researched intensely in the past decade after it was realized that the intrinsic contribution (IC) could be interpreted in terms of the Berry phases of Bloch electrons in a solid [2, 3]. For almost ten years the IC was the only one, which could be accessed in density functional theory (DFT) calculations of the AHE [4–6]. The ability to estimate the impurity-driven (i.e. extrinsic) contributions to the AHE has been remarkably limited so far, thus hindering the predictive power in understanding and engineering the AHE transport properties of real materials.

Besides the IC, σ^{int} , there are two extrinsic disorder-driven contributions to the anomalous Hall conductivity (AHC). In metallic systems they can be distinguished according to their parametric dependency on the impurity concentration n , with skew-scattering conductivity, σ^{sk} , proportional to $1/n$ [7], and the *side-jump* contribution (SJC), σ^{sj} , independent of impurity concentration [8]. The fact that the SJC, although originating from impurities, does not depend on their concentration, makes it one of the most challenging electron scattering mechanisms to understand and suggests a close relation to the intrinsic contribution of the AHE. This behavior arises in metallic systems from the $1/\epsilon_{FT}$ expansion of the transport coefficients in linear response for coupled multi-band systems. Consequently, since the SJC does not depend on the disorder strength, it cannot be easily separated from the IC in low temperature dc measurements [3]. So far, only for an L1₀-ordered FePd ferromagnetic alloy clear evidence has been presented that the side-jump contribution can dominate over other mechanisms of the AHE in a wide temperature range through a comparison of theoretical IC and experimentally measured AHC [9].

Previous numerical *ab initio* treatments have mainly concentrated on the IC [3] and defined the SJC by taking the zero disorder limit of coherent potential approxi-

mation disordered alloys calculations [10]. Within such a treatment the indirect computation of the SJC presents a significant computational challenge considering also that the exact knowledge of the disorder potential in the system is necessary in this case. Since very often the experimental data are obtained on samples with unknown impurity content and disorder type, it is highly desirable to be able to evaluate the SJC explicitly from the electronic structure of a perfect crystal. A direct computation of the SJC in models with disorder was not feasible until recently when it was shown that, assuming short-range uncorrelated disorder model, the SJC may be indeed calculated directly from the ideal electronic structure of a crystal without any disorder [11], rendering possible a rigorous numerical study that can be fully compared to experimental results and can set the stage to a truly predictive theory of the AHE. While the validity of derived expressions has been demonstrated for simple models, values for the *scattering-independent* SJC in fundamental ferromagnetic materials such as Fe, Co or Ni, have not been obtained so far.

In this Letter we report on calculations from first principles of the values of the scattering-independent side-jump conductivity in elemental bcc Fe, hcp Co, fcc Ni, as well as ordered FePd and FePt alloys directly from the electronic structure of their pristine crystals. Our calculations unambiguously show that the calculated values of the total scattering-independent contributions, IC and SJC, agree systematically with experiments to a level that was not reached before in these materials. More importantly, the inclusion of the scattering-independent SJC accounts consistently for the discrepancy between the IC and the measured values in a very non-trivial fashion. We analyze the side-jump as a Fermi surface property and demonstrate that it shows a strong anisotropy with respect to the magnetization direction in the crystal, even more pronounced than that found for the intrinsic AHC [12, 13]. Additionally, we demonstrate the impor-

tance of correlation effects in describing the AHE in fcc Ni correctly.

The starting point for the theory of the scattering-independent side-jump [11] are the retarded Green's function in equilibrium and the Hamiltonian H of a general multiband noninteracting system in three spatial dimensions. At the first step we expand the self-energy of the system Σ_{eq} in powers of potential $V(\mathbf{r})$, which describes scattering at impurities. For a short-range scattering disorder model, scalar delta-correlated Gaussian disorder or delta-scattering uncorrelated disorder, the contribution to the self-energy which is of first order in $V(\mathbf{r})$ vanishes, since one can assume that $\langle V(\mathbf{r}) \rangle = 0$ or else absorb $\langle V(\mathbf{r}) \rangle$ into the Hamiltonian, a procedure which results in a simple shift of the energy levels. Further, inserting the expression for the self-energy within these simple disorder models into appropriate equations for the current densities derived following the Kubo-Středa formalism, rotating into eigenstate representation and keeping only the leading order terms in the limit of vanishing disorder parameter \mathcal{V} , i.e. ignoring skew-scattering contributions, the scattering-independent part of the AHE conductivity may be written as $\sigma^{(0)} = \sigma^{\text{int}} + \sigma^{\text{sj}}$, where

$$\sigma_{ij}^{\text{int}} = \frac{e^2}{\hbar} \int \frac{d^3k}{(2\pi)^3} \text{Im} \sum_{n \neq m} (f_n - f_m) \frac{v_{nm,i}(\mathbf{k})v_{mn,j}(\mathbf{k})}{(\omega_n - \omega_m)^2} \quad (1)$$

can be recovered as the intrinsic contribution [4]. In this expression indices n and m run over all bands with occupations f_n and f_m , respectively, $v_{nm,i}$ are the matrix elements of the velocity operator $\hat{v}_i = \partial_{\hbar k_i} \hat{H}$, and $\omega_n(\mathbf{k}) = \varepsilon_n(\mathbf{k})/\hbar$ with $\varepsilon_n(\mathbf{k})$ as band energies. The scattering-independent SJC to conductivity $\sigma^{(0)}$ reads for inversion-symmetric systems:

$$\sigma_{ij}^{\text{sj}} = \frac{e^2}{\hbar} \sum_n \int \frac{d^3k}{(2\pi)^3} \text{Re} \text{Tr} \left\{ \delta(\varepsilon_F - \varepsilon_n) \frac{\gamma_c}{[\gamma_c]_{nn}} \times \left[S_n A_{k_i} (1 - S_n) \frac{\partial \varepsilon_n}{\partial k_j} - S_n A_{k_j} (1 - S_n) \frac{\partial \varepsilon_n}{\partial k_i} \right] \right\}. \quad (2)$$

Here ε_F is the Fermi energy and the imaginary part of the self-energy $\text{Im}\Sigma_{\text{eq}} = -\hbar\mathcal{V}\gamma$ is taken to be in the eigenstate representation, i.e. $\gamma_c = U^\dagger \gamma U$, with

$$\gamma = \frac{1}{2} \sum_n \int \frac{d^3k}{(2\pi)^2} U S_n U^\dagger \delta(\varepsilon_F - \varepsilon_n), \quad (3)$$

U as the \mathbf{k} -dependent unitary matrix that diagonalizes the Hamiltonian at point \mathbf{k} ,

$$[U^\dagger H(\mathbf{k})U]_{nm} = \varepsilon_n(\mathbf{k})\delta_{nm}, \quad (4)$$

S_n is a matrix that is diagonal in the band indices, $[S_n]_{ij} = \delta_{ij}\delta_{in}$, and the so-called Berry connection matrix is given by $A_{\mathbf{k}} = iU^\dagger \partial_{\mathbf{k}} U$ [11]. Not included in expression (2) are the vertex corrections, which vanish

TABLE I: Anomalous Hall conductivities for bcc Fe and hcp Co in units of S/cm for selected high-symmetry orientations of the magnetization. σ^{int} , σ^{sj} and $\sigma^{\text{int+sj}}$ stand for IC, SJC and their sum, respectively. The experimental values are for the scattering-independent conductivity.

Fe	[001]	[111]	[110]	Co	<i>c</i> axis	<i>ab</i> plane
σ^{int}	767	842	810	σ^{int}	477	100
σ^{sj}	111	178	141	σ^{sj}	217	-30
$\sigma^{\text{int+sj}}$	878	1020	951	$\sigma^{\text{int+sj}}$	694	70
Exp. [20]	1032			Exp. [12]	813	150

for an inversion-symmetric system in the Gaussian disorder model. However, note that in contrast to the original formula as presented in Eq. (3) of Ref. [11], our expression for σ_{ij}^{sj} is manifestly antisymmetric. For the Rashba model it reduces to the original form of Eq. (3) in Ref. [11]. It is important to note that the SJC in the short-range disorder model, Eq. (2), is solely determined by the electronic structure of the pristine crystal and thus directly accessible by *ab initio* methods.

In practice, we replace the integrals in Eqs. (1) and (2) by a discrete sum over a finite number of k -points in the Brillouin zone (BZ). To reduce the computational cost we adopt the method of Wannier interpolation [5, 14], which employs the description of the electronic structure in terms of maximally-localized Wannier functions (MLWFs), to evaluate Eqs. (1) and (2) for bcc Fe, hcp Co, fcc Ni, as well as L1₀ FePd and FePt. The electronic structure calculations were performed with full-potential linearized augmented plane-wave method as implemented in the Jülich DFT code FLEUR [15] within the generalized gradient approximation (GGA). We used the plane-wave cut-off K_{max} of 4.0 bohr⁻¹ and 16000 k -points for self-consistent calculations. Spin-orbit coupling was included in the calculations in second variation. We constructed a set of 18 MLWFs per atom using the Wannier90 code [16] and our interface between FLEUR and Wannier90 [17].

We present the results of our calculations of the intrinsic and side-jump AHC for Fe, Co, Ni, FePd and FePt in Tables I, II, and Fig. 1 for high-symmetry directions of the magnetization \mathbf{M} in the crystal. These results are compared to experimental values, from which the skew scattering contribution was either explicitly subtracted [9, 18], or can be safely ignored at higher temperatures [12, 19, 20].

We first analyze the results for bcc Fe. For \mathbf{M} along [001], the IC in Fe accounts to roughly 75% of the known experimental value of ≈ 1000 S/cm [6, 20]. This comparison gets slightly improved considering that the experimental value averages over crystals with different orientation. Taking the SJC into consideration improves the value of the AHC in Fe significantly for all magnetization directions, with the angle-averaged $\sigma^{\text{int}} + \sigma^{\text{sj}}$ of about 90% of the experimental conductivity. In hcp Co, the magnitude of the SJC for \mathbf{M} along the c axis is as large

as 217 S/cm, with the total AHC of 694 S/cm, very close to the experimental value of about 800 S/cm. For \mathbf{M} in the basal ab plane the SJC is small and negative, bringing thus the intrinsic value down to ≈ 70 S/cm, somewhat away from the experimental value of about 150 S/cm. One has to keep in mind, however, that the experimental values for hcp Co are approximate [12].

A significant improvement upon including the SJC is also evident for the more complex ordered FePd and FePt alloys in their $L1_0$ phase with \mathbf{M} along the [001] axis. For FePd, the IC is very small, of about 130 S/cm, while the side-jump AHC is twice as large and of the same sign, resulting in a value of the total AHC much closer to experiment, Table II. As follows from our calculations, in FePd the AHC is dominated by σ^{sj} , in accordance to an earlier indirect prediction [9]. On the other hand, in FePt with $\mathbf{M}||[001]$, the IC is much larger, while the SJC is half the value of that in FePd. This is again in agreement to Ref. [9], in which such a crossover between the intrinsic and side-jump conductivities, appearing within the Dirac model as well [21], was attributed to different SOI strength of Pd and Pt atoms. As far as the comparison to experiments is concerned, also in FePt adding the calculated SJC to the IC brings the total AHC within the range of experimentally observed values for samples of [001]-magnetized $L1_0$ FePt with high degree of ordering, $S > 0.7$, and different sample thickness [9, 18].

The case of fcc Ni presents a special challenge, since in this material the GGA value of the intrinsic AHC is much larger than the measured scattering-independent value, implying a sizable σ^{sj} with the sign opposite to the IC [6]. From our calculations of the IC in fcc Ni we obtain values which lie between -2000 and -2500 S/cm (Fig. 1 at $U = 0$), depending on the direction of \mathbf{M} , while the experimental value resides in the vicinity of -640 S/cm [6, 22]. The calculated values for the scattering-independent SJC in fcc Ni presented in the same figure (at $U = 0$) lie between -100 and 400 S/cm, and thus cannot explain the large discrepancy between theory and experiment. The description of the electronic structure of Ni within conventional DFT is well-known to be inaccurate, however. Several attempts aiming at improving the GGA values for quantities such as magnetocrystalline anisotropy energy, spin-wave dispersion etc., were made in the past (e.g. Refs. [23], [24] and references therein), proving the importance of correlation effects in this material and the sensitivity of calculated quantities on the shape of its Fermi surface.

TABLE II: Same as in Table I for $L1_0$ FePd and FePt alloys.

FePd	[001]	[110]	FePt	[001]	[110]
σ^{int}	133	280	σ^{int}	818	409
σ^{sj}	263	280	σ^{sj}	128	220
$\sigma^{\text{int+sj}}$	396	560	$\sigma^{\text{int+sj}}$	946	629
Exp. [9]	806		Exp. [9, 18]	900 \div 1267	

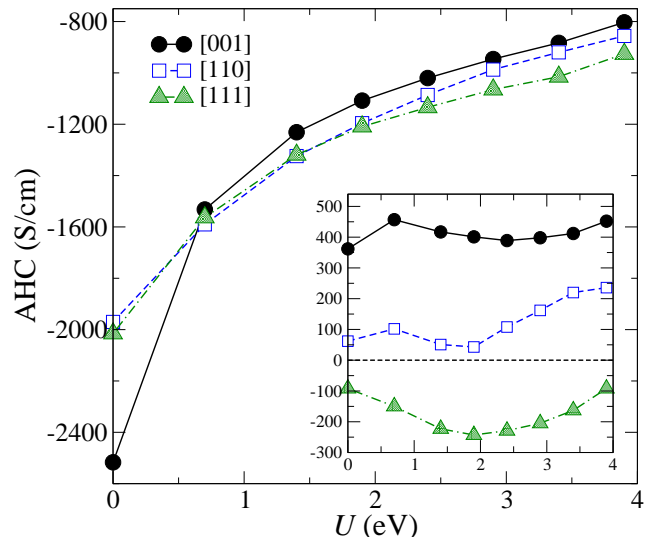


FIG. 1: (Color online) The dependence of the intrinsic and side-jump (inset) conductivities on the strength of the Coulomb repulsion U of valence d -electrons in fcc Ni for different directions of the magnetization in the crystal.

In our work, we choose the GGA+ U approach in order to study the effect of correlations on the AHE in fcc Ni, following the implementation of Ref. [25] and treating the double counting corrections within the atomic limit [26]. For this purpose, we scan the strength of intra-atomic repulsion parameter U , keeping at the same time the intra-atomic exchange parameter J such that the value of the spin moment of Ni stays roughly constant [23]. As can be seen from our calculations, presented in Fig. 1, the values of the σ^{int} upon including U change drastically and come closer to experiment, approaching a value of -800 S/cm when U is changed in the range of 0–4 eV, commonly used for calculations of other properties of Ni [24, 27]. This suggests that the main reason for the discrepancy between the intrinsic AHC values obtained from DFT and experiment might lie in the improper description of Ni’s electronic structure from first principles. On the other hand, the values of the σ^{sj} are affected differently by the modifications in the electronic structure, almost not changing for \mathbf{M} along the [001] axis, and displaying a non-monotonous behavior within the range of 100–300 S/cm in the absolute value as a function of U for two other magnetization directions.

Such different sensitivity to the band structure can be understood by analyzing the structure of the SJC and the IC on the Fermi surface (FS). To simplify things, when taking into account the very complicated FSs of the ferromagnets considered in this study, we sum up the contributions to σ^{int} and σ^{sj} over all bands and all sheets of the FS, respectively, following Eqs. (1) and (2), when going along a certain direction in the BZ until the inner “Fermi” sphere in the BZ with the center at its

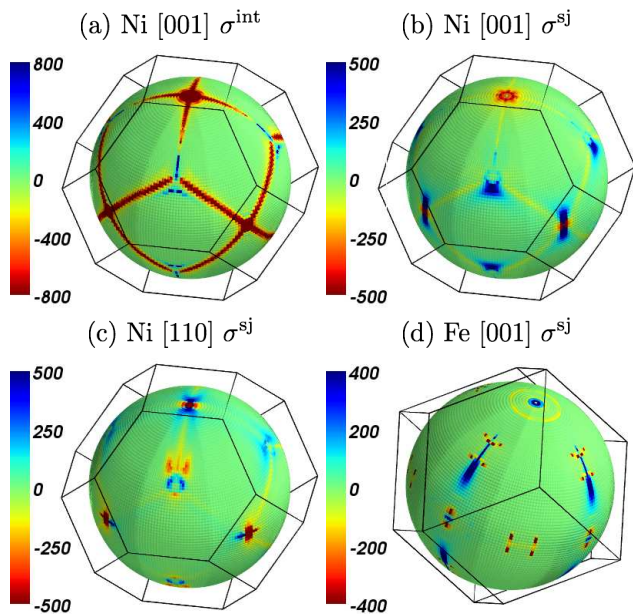


FIG. 2: (Color online) Angle-resolved conductivity $d\sigma/d\Omega$ in units of S/cm as a function of direction in the BZ. $d\sigma/d\Omega$ corresponds to all contributions to σ from inside the inner sphere in the BZ within the solid angle element $d\Omega$. (a) σ^{int} for Ni [001], (b) σ^{sj} for Ni [001], (c) σ^{sj} for Ni [110], (d) σ^{sj} for Fe [001].

origin (Γ -point) is reached. In the case of such angle-resolved IC in Ni ($U = 0$), shown in Fig. 2(a), large contributions can be seen along the "hot loops" in the BZ, which are situated in the vicinity of the intersections between different sheets of bands [13], while the IC in the region away from such band crossings is also significant [6]. This is rather different from the topology of the SJC on the Fermi sphere. The SJC in Ni ($U = 0$) and Fe, presented in Fig. 2(b)-(d) manifests that the main contribution to σ^{sj} comes from certain isolated "hot spots", distributed rather sparsely over the Fermi sphere, while the SJC decays very quickly with the distance from such points. Such a strong difference in the distribution of the σ^{sj} and σ^{int} on the FS arises from the effective magnetic monopole nature of the IC Berry's phase contribution near the band crossings, resulting in a more pronounced sensitivity of the σ^{int} to the parameters of the electronic structure, such as Coulomb repulsion U , Fermi energy etc., whereas the SJC does not contain such singularities near those crossings.

From our calculations presented above in Tables I, II, Figs. 1 and 2, it is evident that σ^{sj} exhibits large changes when the direction of the magnetization in the crystal is varied. In uniaxial crystals, such as FePt and hcp Co such anisotropy is not surprising, given that in these materials also the anisotropy of the intrinsic AHC appears already in the first order with respect to the directional cosines of the magnetization [12]. And while the differ-

ence in the absolute change in the SJC and IC in FePd and FePt upon rotating the magnetization direction can be probably related to different SOI strength of the two materials [9], in FePt the corresponding trend of the SJC and the IC is opposite owing to the different Fermi surface topology of the two contributions. Surprisingly, the strong anisotropy of the SJC can be also observed in bcc Fe and fcc Ni. In Fe this anisotropy reaches as much as 70%, while in Ni the SJC anisotropy is striking as compared to the IC anisotropy, with changes in sign and order of magnitude of σ^{sj} as a function of the magnetization direction. This can be perhaps intuitively understood considering that σ^{sj} is given almost entirely by singular "hot spots" at the FS, which change their position and the magnitude of their contribution depending on the matrix elements of the SOI, controlled in turn by the magnetization direction [12, 28], compare e.g. Fig. 2(b) and (c) for Ni.

Despite the unprecedented improvement of the values of the AHC in several ferromagnets when compared to the experimentally measured numbers, the scattering-independent SJC considered here cannot describe the entire physics of the complex side-jump scattering and will likely fail to describe it in certain systems where long-range scattering and spin-dependent scattering dominate. This can be particularly important for the case of low-doped, i.e., having long screening length, magnetic systems. Also, within our approach, we consider only the leading-order in impurity strength correction to the self-energy, which is justified within the weak scattering limit. This approximation might fail, however, when the perturbation in the crystal potential due to the presence of disorder or impurities is very strong. It would be highly desirable to extend the current model for the scattering-independent side-jump conductivity beyond the short-range disorder and weak scattering limit.

In summary, we have implemented a method to calculate the scattering-independent SJC within DFT. We found that for fundamental ferromagnets, such as Fe, Co, FePd and FePt the agreement between theory and experiment can be essentially improved upon considering the scattering-independent SJC. This SJC can be calculated from the electronic structure of the pristine crystal only, which encourages the application of the considered model for the side-jump scattering to wider classes of materials with the goal of extending the applicability of the DFT in treating complex transverse scattering phenomena and comparison to experiments that are commonly performed on samples with unknown disorder and impurity content.

We gratefully acknowledge Jülich Supercomputing Centre for computing time and funding under the HGF-YIG Programme VH-NG-513. JS was supported under Grant Nos. onr-n000141110780 and NSF-DMR-1105512 and by the Research Corporation Cottrell Scholar Award.

-
- * corresp. author: y.mokrousov@fz-juelich.de
- [1] E. H. Hall, *Philos. Mag.* **12**, 157 (1881)
 - [2] N. Nagaosa, *J. Phys. Soc. Jpn.* **75**, 042001 (2006)
 - [3] N. Nagaosa *et al.*, *Rev. Mod. Phys.* **82**, 1539 (2010)
 - [4] Y. Yao *et al.*, *Phys. Rev. Lett.* **92**, 037204 (2004)
 - [5] X. Wang *et al.*, *Phys. Rev. B* **74**, 195118 (2006)
 - [6] X. Wang *et al.*, *Phys. Rev. B* **76**, 195109 (2007)
 - [7] J. Smit, *Physica* **24**, 39 (1958)
 - [8] L. Berger, *Phys. Rev. B* **2**, 4559 (1970)
 - [9] K. M. Seemann *et al.*, *Phys. Rev. Lett.* **104**, 076402 (2010)
 - [10] S. Lowitzer *et al.*, *Phys. Rev. Lett.* **105**, 266604 (2010)
 - [11] A. A. Kovalev *et al.*, *Phys. Rev. Lett.* **105**, 036601 (2010)
 - [12] E. Roman *et al.*, *Phys. Rev. Lett.* **103**, 097203 (2009)
 - [13] H. Zhang *et al.*, *Phys. Rev. Lett.* **106**, 117202 (2011)
 - [14] J. R. Yates *et al.*, *Phys. Rev. B* **75**, 195121 (2007)
 - [15] For description of the code see <http://www.flapw.de>
 - [16] A. A. Mostofi *et al.*, *Comp. Phys. Comm.* **178**, 685 (2008)
 - [17] F. Freimuth *et al.*, *Phys. Rev. B* **78**, 035120 (2008)
 - [18] M. Chen *et al.*, *Appl. Phys. Lett.* **98**, 082503 (2011)
 - [19] T. Miyasato *et al.*, *Phys. Rev. Lett.* **99**, 086602 (2007)
 - [20] P. N. Dheer, *Phys. Rev.* **156**, 637 (1967)
 - [21] N. A. Sinitsyn *et al.*, *Phys. Rev. B* **75**, 045315 (2007)
 - [22] J. M. Lavine, *Phys. Rev.* **123**, 1273 (1961)
 - [23] I. Yang *et al.*, *Phys. Rev. Lett.* **87**, 216405 (2001)
 - [24] E. Şaşıoğlu *et al.*, *Phys. Rev. B* **81**, 054434 (2010)
 - [25] A. Shick *et al.*, *Phys. Rev. B* **60**, 10763 (1999)
 - [26] For several values of the parameter U we compared our results to the values of the AHC obtained in the "around mean field" limit, and did not find significant changes in the AHC.
 - [27] For bcc Fe applying a GGA+ U approach with parameter U of up to 2 eV results in a smooth positive shift of the values of the IC and SJC by up to approximately 60 and 40 S/cm, respectively, for all magnetization directions, bringing thus the total value of the calculated AHC even closer to experiment.
 - [28] K. Hals *et al.*, *Phys. Rev. Lett.* **105**, 207204 (2010)